ELSEVIER

Biochimica et Biophysica Acta 1194 (1994) 75–91

BBA Biochimica et Biophysica Acta

Changes of protein structure, nucleotide microenvironment, and Ca^{2+}-binding states in the catalytic cycle of sarcoplasmic reticulum Ca^{2+}-ATPase: investigation of nucleotide binding, phosphorylation and phosphoenzyme conversion by FTIR difference spectroscopy

Andreas Barth *, Werner Kreutz, Werner Mäntele

Institut für Biophysik und Strahlenbiologie der Universität Freiburg, Albertstr. 23, D-79104 Freiburg, Germany

Received 5 October 1993; revised 28 February 1994

Abstract

Changes of infrared absorbance of sarcoplasmic reticulum Ca^{2+}-ATPase (EC 3.6.1.38) associated with partial reactions of its catalytic cycle were investigated in the region from 1800 to 950 cm^{-1} in H_2O and ^2H_2O. Starting from Ca_2E_1, 3 reaction steps were induced in the infrared cuvette via photolytic release of ATP and ADP: (a) nucleotide binding, (b) formation of the ADP-sensitive phosphoenzyme (Ca_2E_1P) and (c) formation of the ADP-insensitive phosphoenzyme (E_2P). All reaction steps caused distinct changes of the infrared spectrum which were characteristic for each reaction step but comparable for all steps in the number and magnitude of the changes. Most pronounced were absorbance changes in the amide I spectral region sensitive to protein secondary structure. However, they were small – less than 1% of the total protein absorbance – indicating that the reaction steps are associated with small and local conformational changes of the polypeptide backbone instead of a large conformational rearrangement. Especially, there is no outstanding conformational change associated with the phosphoenzyme conversion $Ca_2E_1P \rightarrow E_2P$. ADP-binding induces conformational changes in the ATPase polypeptide backbone with α-helical structures and presumably β-sheet or β-turn structures involved. Phosphorylation is accompanied by the appearance of a keto group vibration that can tentatively be assigned to the phosphorylated residue Asp^{351}. Phosphoenzyme conversion and Ca^{2+}-release produce difference signals which can be explained by the release of Ca^{2+} from carboxylate groups and a change of hydrogen bonding or protonation state of carboxyl groups.

Key words: Infrared spectroscopy; ATPase, Ca^{2+}-; Sarcoplasmic reticulum; Structure; Structural change

1. Introduction

Active Ca^{2+}-transport from the cytoplasm of muscle cells across the sarcoplasmic reticulum membrane is essential for muscle relaxation. It is performed by the Ca^{2+}-ATPase, an intrinsic membrane protein, that couples ATP-hydrolysis to Ca^{2+}-transport. Although the ATPase reaction cycle (Fig. 1A) has been the subject of detailed investigations for the past years, the nature of the coupling process is still unknown. The investigation of structural changes that accompany the catalytic cycle of the ATPase should help to get more insight into the coupling process. Of special interest is the phosphoenzyme conversion from Ca_2E_1P to E_2P, where orientation and affinity of the Ca^{2+}-binding sites and the reactivity towards ADP are changed. Several observations indicate that this step is connected with a structural change, but there is evidence that no major rearrangement of the ATPase occurs (see references in [1] and [2]). For lack of a high-resolution structure of the ATPase, the exact structure of the binding site as

Abbreviations: Ca_2E_1P, ADP-sensitive phosphoenzyme; E_2P, ADP-insensitive phosphoenzyme; caged ATP (or ADP), P-1-(2-nitro)phenylethyl ATP (or ADP); δ, deformation vibration; EDTA, (ethylenedinitrilo)tetraacetic acid; EDTA·Ca^{2+}, Ca^{2+} complex of EDTA; FTIR, Fourier transform infrared; IR, infrared; ν_{as}, asymmetric stretch vibration; ν_s, symmetric stretch vibration; Me_2SO, dimethylsulfoxide; Mops, 3-(*N*-morpholino)propanesulfonic acid; Nitr-5, 1,2-amino-5-[1-hydroxy-1-(2-nitro-4,5-methylenedioxyphenyl) methyl]phenoxyl-2-(2′-amino-5′-methylphenoxy)ethane-*N,N,N′,N′*-tetraacetic acid tetrasodium salt; OD, dimensionless absorbance unit; SR, sarcoplasmic reticulum.

* Corresponding author. Fax: +49 761 2035016.

SSDI 0005-2736(94)00125-9

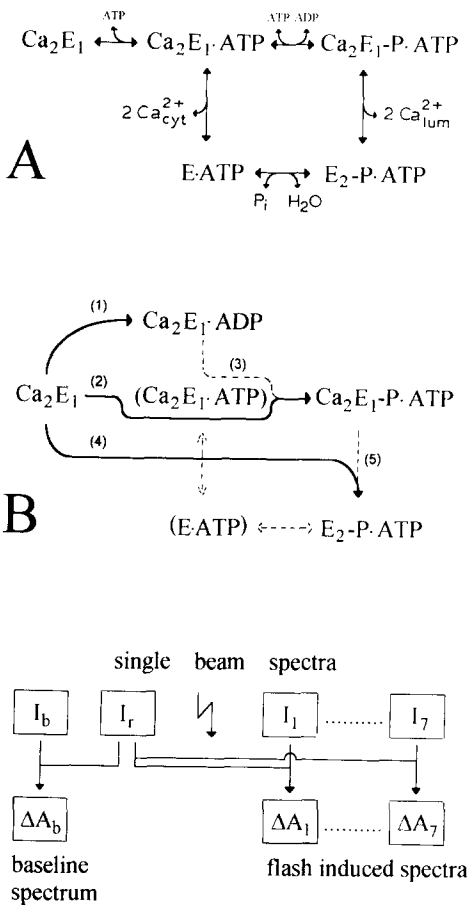

Fig. 1 (A) Reaction cycle of the Ca^{2+}-ATPase (modified from [1,54]). Cyt, cytoplasm; lum, SR lumen. (B) Reaction steps investigated by IR difference spectroscopy. Bold lines: steps directly induced in the IR cuvette. Dashed lines: spectra of these steps were calculated by subtraction of difference spectra. Dotted lines: steps not investigated. (C) Flow diagram of spectra recording and calculation. The arrow symbolizes the photolysis flash.

well as structural details necessary for the Ca^{2+} transport mechanism remain speculative. Furthermore, the static picture which an X-ray structure might provide would not give sufficient information on the conversion of the phosphoenzyme; mechanistic information thus relies mostly on spectroscopic data.

Infrared (IR) spectroscopy can be used to follow small structural changes associated with nucleotide binding and ATPase phosphorylation, provided that reaction-induced-difference-techniques are applied [2,3]. With these techniques, a sample and a reference spectrum are recorded from the same sample in rapid succession, with a suitable perturbation applied in between to start the desired reaction. Thus, from the spectra before and after the perturbation, a difference spectrum can be calculated that reflects only those changes of IR absorption which are associated with the reaction. Negative bands of the difference spectrum are characteristic for the initial state, positive bands for the intermediate state or the final product. The accuracy of this method is extremely high, since the difference spectrum is not obtained by subtraction of spectra from samples prepared under different conditions (which would lead to inaccuracies arising from variations of sample concentration and cell pathlength). The detection limit for our samples in the amide I spectral region, sensitive to protein secondary structure, is an absorbance change of much less than 0.1% of total protein absorbance. While this technique of reaction-induced-IR-difference-spectroscopy had been originally developed for the study of photoreactive proteins which can be stimulated by light absorption, application to the study of substrate/cofactor binding to enzymes and to enzyme reactions in general seemed difficult.

Recently, we have reported the use of photolabile substrate analogues ('caged substrates') in combination with Fourier transform infrared (FTIR) difference spectroscopy and were able to show that ATPase samples which hydrolize ATP and perform Ca^{2+}-transport can be prepared at the low H_2O content needed for IR measurements in the mid IR region (1800 – 950 cm^{-1}) [2,3]. Photolytic release of ATP in these samples produced IR absorbance changes that could be assigned to photolysis of caged ATP, hydrolysis of ATP and to formation of the ADP-sensitive phosphoenzyme ($Ca_2E_1 \rightarrow Ca_2E_1P$) in H_2O and ^2H_2O. While the aim of our preceding papers was mainly to present this IR-spectroscopic method, we here report the investigation of 3 essential steps of the Ca^{2+}-ATPase reaction cycle: (i) nucleotide (ADP) binding (step (1) in Fig. 1B), (ii) formation of the ADP-sensitive phosphoenzyme ($Ca_2E_1 \rightarrow Ca_2E_1P$, step (2) in Fig. 1B), and (iii) formation of the ADP-insensitive phosphoenzyme ($Ca_2E_1 \rightarrow E_2P$, step (4) in Fig. 1B). These reaction steps result in IR absorbance changes which we have investigated in H_2O and ^2H_2O in the region from 1800 to 950 cm^{-1}. The obtained difference spectra were normalized and compared in order to separate the processes of nucleotide binding, phosphorylation and phosphoenzyme conversion.

2. Experimental procedures

2.1. Sample preparation and sample terminology

Ca^{2+}-ATPase prepared according to De Meis and Hasselbach [4] was a generous gift of W. Hasselbach (Max-Planck-Institut für medizinische Forschung, Heidelberg, Germany). Table 1a lists the composition of samples for IR spectroscopy which were prepared as described in [2] for the investigation of different reaction steps. Briefly, SR vesicles were dialysed overnight

at 5°C in 20 mM 3-(*N*-morpholino)propanesulfonic acid (Mops)/KOH (pH or pD 7), 10 mM KCl or LiCl, 0.2 or 1 mM $MgCl_2$ and 10 μM $CaCl_2$. After adding the substances to give the final concentrations listed in Table 1a, 15 μl of SR-solution were dehydrated under controlled conditions on a CaF_2 IR-window, and then sealed with a second window. In order to remove Na^+ from the caged ATP stock solution, the solution was dialyzed 30 min in a dialysis membrane with small pores (molecular weight cutoff 100, Medical Industries, Los Angeles, CA, USA) for the K^+-free samples. Samples are named according to the reaction investigated (for example $Ca_2E_1 \rightarrow Ca_2E_1P$-sample for the investigation of the reaction $Ca_2E_1 \rightarrow Ca_2E_1P$). Two kinds of samples were prepared to investigate each of the phosphoenzymes Ca_2E_1P and E_2P. In the one type (named $Ca_2E_1 \rightarrow Ca_2E_1P$-sample and $Ca_2E_1 \rightarrow E_2P$-sample) the decay of the respective phosphoenzyme was rate limiting, but the ATP-hydrolyzing activity was high enough that all released ATP reacted within the time of the experiment (4 min). In the other type (named $Ca_2E_1 \rightarrow Ca_2E_1P$-(high Ca^{2+})-sample and $Ca_2E_1 \rightarrow E_2P$-(+Me_2SO)-sample), phosphoenzyme decay and therefore ATP hydrolysis was inhibited and the phosphoenzyme of interest accumulated to a higher extent as compared to the first type (see Discussion). Samples to investigate the photolysis reaction were prepared in the same way, but, instead of drying an ATPase solution, only caged ATP or caged ADP together with 15 μl of dialyzing buffer were dried.

2.2. Experiments in ^2H_2O

SR membranes were first dialysed for 1 h in H_2O-buffer and then 15–20 h in ^2H_2O-buffer of the same composition at 5°C. Samples were dried until free water was almost completely removed and then rehydrated with 0.5–1 μl ^2H_2O with or without 20% Me_2SO.

2.3. Estimation of protein content of the samples

Protein content was estimated from the amide I and amide II protein absorbance as described in [2] using for samples in H_2O the amide II band (absorbance difference between 1544 and 1490 cm^{-1}, calibration factor 690 $\mu g\,cm^{-2}\,OD^{-1}$) and for samples in ^2H_2O the amide I band (absorbance difference between 1704 and 1646 cm^{-1}, calibration factor 375 $\mu g\,cm^{-2}\,OD^{-1}$).

2.4. FTIR measurements

FTIR measurements were performed with a Bruker IFS 25 instrument equipped with a HgCdTe detector of selected sensitivity. For the difference measurements 9 subsequent single beam spectra (I_b, I_r, I_1 to

Table 1a
Approximate concentrations of ATPase, cofactors and other constituents in the ATPase samples

Sample name	ATP-ase (mM)	Mops (mM)	pH, pD	K^+ (mM)	Li^+ (mM)	Mg^{2+} (mM)	Ca^{2+} (mM)	Glu-ta-thione (mM)	Caged ATP or ADP (mM)	A23187 (mg/ml)	Other
ADP-binding	1	300	7.0	330	–	3	0.15	10–40	10–40	–	–
$Ca_2E_1 \rightarrow Ca_2E_1P$	1	300	7.0	330	–	3	0.15	10	10	–	–
$Ca_2E_1 \rightarrow Ca_2E_1P$-(high Ca^{2+})	1	300	7.0	330	–	3	20	10	10	0.5	–
$Ca_2E_1 \rightarrow E_2P$ (only in H_2O)	1	300	7.0	–	260	15	0.15	10	6–12	0.5	–
$Ca_2E_1 \rightarrow E_2P$-(+Me_2SO)	1	300	7.0	–	260	15	0.15	10	6–12	0.5	20% Me_2SO

Based on 1 μl sample volume and on 4.5 nmol ATPase/mg protein [53].

Table 1b
Spectra terminology

Name of spectrum	Meaning
Flash-induced spectra	ΔA_x (see Fig. 1C)
Photolysis spectra	ΔA_x of samples not containing ATPase
ADP-binding-spectra $Ca_2E_1 \rightarrow Ca_2E_1P$-spectra or $Ca_2E_1 \rightarrow E_2P$-spectra $Ca_2E_1 \rightarrow Ca_2E_1P$-transient-spectra or $Ca_2E_1 \rightarrow E_2P$-transient-spectra	ΔA_x minus photolysis spectrum early ΔA_x minus late ΔA_y, for example ΔA_x–ΔA_7
Phosphorylation spectrum	normalized $Ca_2E_1 \rightarrow Ca_2E_1P$-spectrum minus normalized ADP-binding-spectrum
$Ca_2E_1P \rightarrow E_2P$ spectrum	normalized $Ca_2E_1 \rightarrow E_2P$-spectrum minus normalized $Ca_2E_1 \rightarrow Ca_2E_1P$-spectrum

I_7) were recorded between 1800 and 900 cm^{-1}. Between I_r and I_1, photolysis was triggered by a Xenon flash tube as described in [2] (see Fig. 1C for a flow diagram of spectra recording). Spectra were calculated from 100 averaged interferometer scans per spectrum except for I_b, I_1 and I_2, which were calculated from 20 (I_b and I_1) or 50 scans (I_2), respectively, in order to achieve a better time resolution immediately after the flash and to compare I_b with I_1. Data acquisition for the spectra after the flash took place in the following time intervals: I_1: 0–8 s; I_2: 16–34 s; I_3: 42–74 s; I_4: 82–114 s; I_5: 122–154 s; I_6: 162–194 s; I_7: 202–234 s. The absorbance difference between the reference spectrum I_r, recorded immediately before the flash, and the other spectra I_x was obtained by calculating $\Delta A_x = -\log(I_x/I_r)$. This is a more direct expression for the difference spectrum than subtraction of the respective absorbance spectra. The difference spectrum ΔA_b calculated from the spectra recorded before the flash served as baseline control. The others showed the absorbance changes after application of the flash. All spectra were recorded at 1°C with 4 cm^{-1} resolution and triangular apodization.

2.5. Subtraction procedures and spectra terminology

Difference spectra ΔA_1 to ΔA_7, directly obtained from the IR measurements of ATPase samples, are named flash-induced-spectra (see Table 1b for a short description of the spectra terminology). Difference bands which can be attributed to the processes of photolysis or hydrolysis or to structural changes in the ATPase-nucleotide-complex are named photolysis bands, hydrolysis bands or ATPase-nucleotide-bands, respectively. For each ATPase sample, the difference spectrum of the photolysis reaction was investigated separately in the same buffer, but in the absence of ATPase. Then this photolysis spectrum was normalized to the flash-induced-spectra using the photolysis bands at 1524, 1346 and below 1300 cm^{-1} [2,3]. However, these photolysis bands were partly superimposed by hydrolysis bands or ATPase-nucleotide-bands. Hydrolysis bands are smallest in the first flash-induced-spectrum ΔA_1 due to the short time between ATP release and spectra acquisition, and ATPase-nucleotide-bands are smallest in the last flash-induced-spectrum ΔA_7 provided that the decay of the ATPase-nucleotide-bands could be observed ($Ca_2E_1 \rightarrow Ca_2E_1P$-samples and $Ca_2E_1 \rightarrow E_2P$-samples). Therefore, in the case of overlap by hydrolysis bands (below 1300 cm^{-1}), the photolysis spectrum should fit well to the first flash-induced-spectrum ΔA_1. In the case of overlap by ATPase-nucleotide-bands, it should fit to the last flash-induced-spectrum ΔA_7. The normalized photolysis spectrum was subtracted from the flash-induced-spectra. The resulting spectra show mainly the ATPase-nucleotide-bands. Therefore these difference spectra and their ATPase-nucleotide-bands are named according to the reaction step investigated, for example $Ca_2E_1 \rightarrow Ca_2E_1P$-spectra and $Ca_2E_1 \rightarrow Ca_2E_1P$-bands. These spectra have to be interpreted cautiously, because the presence of SR may change position and intensity of the photolysis bands which may lead to incomplete subtraction and therefore to artificial difference bands in the region of photolysis bands which cannot be attributed to ATPase-nucleotide-bands.

For the investigation of phosphoenzyme formation, a second independent way of subtracting the photolysis bands was used. With appropriate sample compositions, the ATP-hydrolizing activity of the samples was high enough to consume all of the released ATP within the time of the experiment. Thus, while the phosphoenzyme decomposes, the decay of bands arising from phosphoenzyme formation could be observed. This was used to calculate transient-spectra. These spectra show the difference between the transient state shortly after ATP release and the final state, and were obtained by subtracting one of the later flash-induced-spectra from the preceding (for example ΔA_x minus ΔA_7). In this way photolysis bands cancel out and ATPase-nucleotide-bands as well as hydrolysis bands are retained. As compared to the procedure of subtracting a photolysis spectrum, hydrolysis bands have the opposite sign in the transient-spectra, thus facilitating the distinction between hydrolysis- and ATPase-nucleotide-bands.

2.6. Normalization of IR difference spectra to a uniform protein content

In order to compare the difference spectra of the three investigated reactions, they were normalized to a uniform protein content. First, the linear dependence of the protein difference bands from the protein content of the samples was verified. A suitable band is the 1624 cm^{-1} band which appears upon ADP-binding and phosphoenzyme formation [2] and is not very sensitive to phosphoenzyme conversion (see Results section). This band was chosen because of its high intensity and because it is located sufficiently away from the strongest water and protein absorption range (around 1650 cm^{-1}) where baseline instabilities may occur. A linear dependence of the 1624 cm^{-1} band on the protein content could be established for most of the samples (data not shown). However, some of the samples showed a smaller 1624 cm^{-1} band. This may be due to sample inhomogeneities (small air bubbles) which can lead to a deviation from Lambert-Beer's law. In the case of Me_2SO-containing-samples, a reduced 1624 cm^{-1} band may be due to the development of a critically high Me_2SO concentration during sample preparation, which leads to irreversible inhibition of Ca^{2+}-ATPase [5]. For the normalized difference spectra, only sam-

ples following the linear relation betweeen the protein content and the 1624 cm^{-1} band amplitude were used. Spectra were first normalized to a protein content of 180 $\mu g/cm^2$ (corresponding to an amide I absorbance of 0.48 OD and to an amide II absorbance of 0.26 OD) and then averaged.

3. Results

3.1. Binding of ADP to Ca_2E_1

Fig. 2 shows IR difference spectra arising from the release of ADP from caged ADP in ATPase samples. ADP-binding-spectra (thin lines in Fig. 2) reflecting reaction step (1) in Fig. 1B could be obtained by subtraction of the photolysis spectrum of caged ADP (dotted lines in Fig. 2). Bands which are obvious in the flash-induced-spectra (thick lines) and absent in the photolysis spectra (dotted lines) arise from ADP binding to the ATPase and are called ADP-binding-bands. Their position is shown in Table 2. The size of the ADP-binding-bands in H_2O and ^2H_2O was comparable to the size of the ATP-induced ATPase-nucleotide-bands (see Fig. 5). However, to obtain saturation of the amplitude for the ADP-binding-bands, more ADP had to be released as compared to the amount of ATP necessary for the saturation of the amplitudes of the bands of phosphoenzyme formation. In the regions of the photolysis bands around 1524, 1344 and below 1250 cm^{-1} [2,3] the attribution of difference bands observed in the flash-induced-spectra (thick lines) to ADP-binding-bands is difficult (see Experimental procedures section). However, the negative band around 1200 cm^{-1} in H_2O and ^2H_2O (Figs. 2A and C) leads to a significant modification of the shape of the flash-induced-spectrum when compared to the photolysis spectrum, and is therefore attributed to ADP-binding.

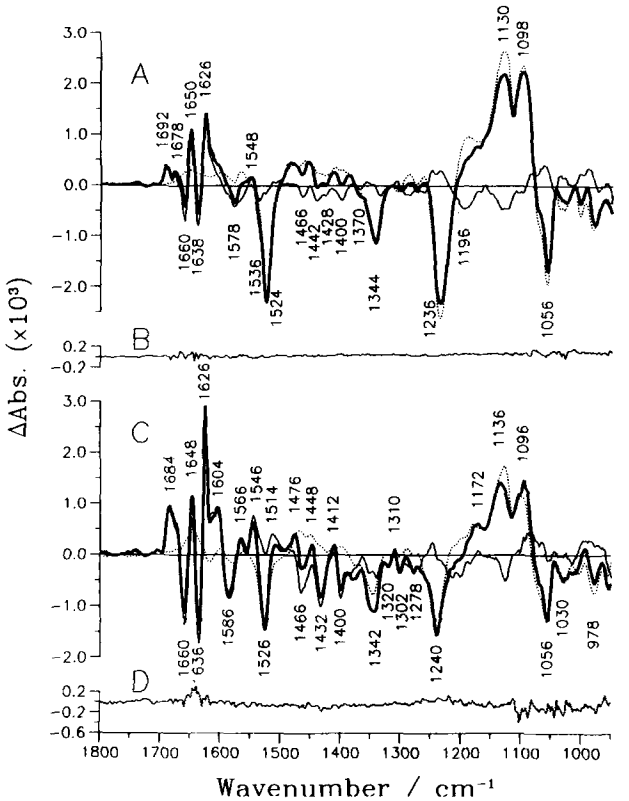

Fig. 2. IR difference spectra after release of ADP in ADP-binding samples in H_2O and ^2H_2O. $T = 1°C$. The numbers give the band positions of the bold and thin line spectra. (A) Spectra in H_2O, average of four samples. Bold line: average of flash-induced-spectra ΔA_2 to ΔA_5. Thin line: ADP-binding-spectrum. Dotted line: Photolysis spectrum of caged ADP. (B) Baseline spectrum ΔA_b of the ADP-binding-samples in H_2O. (C) Spectra in ^2H_2O, average of two samples. Bold line: average of flash-induced-spectra ΔA_1 to ΔA_4. Thin line: ADP-binding-spectrum. Dotted line: Photolysis spectrum of caged ADP in ^2H_2O. (D) Baseline spectrum ΔA_b of the ADP-binding-samples in ^2H_2O.

Table 2
ADP-binding-bands arising from binding of ADP to Ca_2E_1.

H_2O	D_2O	H_2O	D_2O
1692 (+)	1684 (+)	1466 (−)	1466 (−)
1678 (+)		1442 (−)	1432 (−)
1660 (−)	1660 (−)	1428 (−)	
1650 (+)	1648 (+)	1400 (−)	1400 (−)
1638 (−)	1636 (−)	1370 (−)(?)	
1626 (+)	1626 (+)		1320 (−)(?)
	1604 (+)		1310 (+)(?)
1578 (−)	1586 (−)		1302 (−)(?)
	1566 (+)		1278 (−)(?)
1548 (+)(?)	1546 (+)	1196 (−)	~1200 (−)
1536 (−)(?)	1514 (+)		

The numbers give the positions of the difference bands in wavenumbers. (?) means that the attribution is not secure, (+) or (−) mean positive or negative band.

When the experiments are performed in ^2H_2O (Fig. 2C) instead of H_2O (Fig. 2A), several distinct alterations in the ADP-binding-spectrum are observed. The double band around 1690 cm^{-1} is shifted by 6–8 cm^{-1} to lower wavenumbers, new bands appear at 1586 and 1566 cm^{-1} (instead of one band at 1578 cm^{-1}), and the double band at 1442 and 1428 cm^{-1} is replaced by a single band at 1432 cm^{-1}. At 1320, 1310, 1302 and 1278 cm^{-1} small bands appear in ^2H_2O, which cannot unambiguously be attributed to ADP-binding-bands because of their small amplitude. The samples in ^2H_2O show stronger ADP-binding-bands than the samples in H_2O in spite of their lower protein content.

3.2. Formation of Ca_2E_1P from Ca_2E_1 in H_2O

$Ca_2E_1 \rightarrow Ca_2E_1P$-samples (investigation of step (2) in Fig. 1B) contained about 330 mM K^+ and 3 mM $MgCl_2$ (cf. Table 1a). They were never dried completely in order to avoid leaky vesicles [6]. Samples prepared in this way were able to accumulate Ca^{2+} in

the vesicles [2]. Thus, Ca^{2+}-transport should lead to a high Ca^{2+}-concentration inside the vesicles in spite of the lower concentration of about 150 μM in the external medium. As a working hypothesis, we assume that the release of ATP in these samples leads to the accumulation of the ADP-sensitive phosphoenzyme (Ca_2E_1P, see discussion section).

Fig. 3 shows absorbance changes due to the release of ATP in these samples. Transient absorbance changes due to formation of Ca_2E_1P [2] (best seen in the region 1700–1600 cm^{-1}) are strongest in the first spectrum recorded in the time range 0–8 s after the photolysis flash (bold lines in Fig. 3) and decay within 100 s. Small permanent changes remain (thin lines in Fig. 3) which cannot be explained by the photolysis reaction. These resemble the ADP-binding-spectrum (Fig. 2A) and are therefore attributed to the binding of ADP – as a product of ATP hydrolysis – to the ATPase. After 100 s, the rise of the hydrolysis bands at 1242 and 1090 cm^{-1} [2,3] was complete.

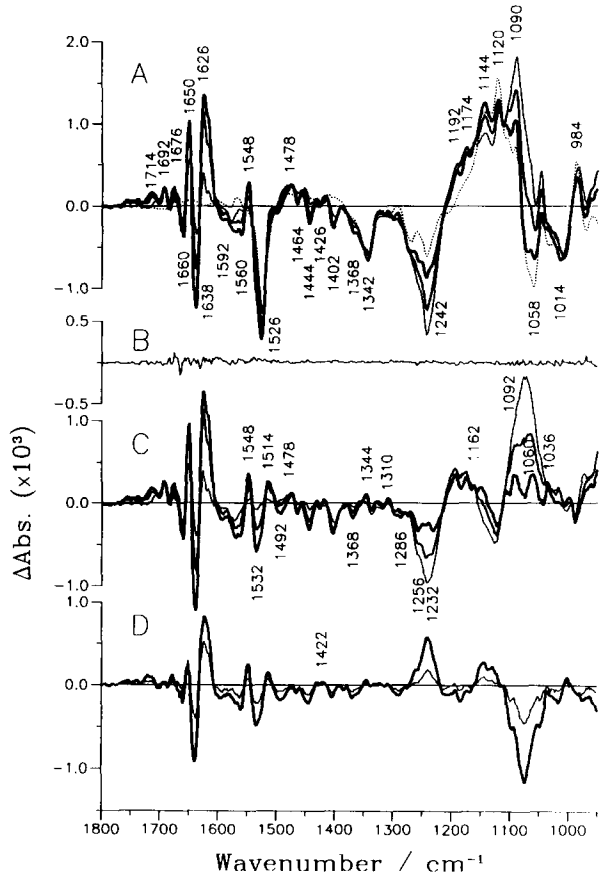

Fig. 3. IR difference spectra after ATP release in $Ca_2E_1 \rightarrow Ca_2E_1P$-samples in H_2O. $T = 1°C$, average of four samples. The numbers give the band positions of the bold line spectra. (A) Full lines: flash-induced-spectra ΔA_x, bold: ΔA_1, medium: ΔA_2, thin: average of ΔA_4 to ΔA_7. Dotted line: Photolysis spectrum. (B) Baseline spectrum ΔA_b. (C) $Ca_2E_1 \rightarrow Ca_2E_1P$-spectra, calculated from bold: ΔA_1, medium: ΔA_2, thin: average of ΔA_4 to ΔA_7. (D) $Ca_2E_1 \rightarrow Ca_2E_1P$-transient-spectra: flash-induced-spectra ΔA_x minus ΔA_3, bold: ΔA_1, thin: ΔA_2.

Table 3
$Ca_2E_1 \rightarrow Ca_2E_1P$-bands of the $Ca_2E_1 \rightarrow Ca_2E_1P$-samples

H_2O	D_2O	H_2O	D_2O
1750 (+)	1740 (+)	1402 (−)	1400 (−)
1714 (+)	1706 (+)		1382 (−)
1692 (+)	1686 (+)	1368 (−)	1374 (−)
1676 (+)	1670 (+)		1352 (−)
1660 (−)	1660 (−)	1344 (+)	1344 (+)(?)
1650 (+)	1648 (+)		1330 (+)
1638 (−)	1638 (−)	1310 (+)	1308 (+)
1626 (+)	1626 (+)	1286 (−)	
1592 (−)	1588 (−)	1256 (−)(?)	1256 (−)(?)
1560 (−)	1560 (−)	1232 (−)(?)	
1548 (+)	1546 (+)	1192 (+)	1188 (+)
1532 (−)	1526 (−)	1174 (+)	1172 (+)
1514 (+)	1514 (+)	1162 (+)(?)	
1492 (−)	1484 (+)	1144 (+)(?)	1148 (+)(?)
1464 (−)	1466 (+)	1122 (−)(?)	
1444 (−)	1436 (−)	1092 (+)	1092 (+)
1430 (+)(?)		1060 (+)	1062 (+)
1426 (−)(?)	1418 (+)		
1422 (+)(?)			

The numbers give the positions of the difference bands in wavenumbers. (?) means that the attribution is not secure, (+) or (−) mean positive or negative band.

Fig. 3C shows the $Ca_2E_1 \rightarrow Ca_2E_1P$-spectra obtained by subtraction of the photolysis spectrum from the flash-induced-spectra (dotted and full lines, respectively in Fig. 3A). The $Ca_2E_1 \rightarrow Ca_2E_1P$-spectra have to be interpreted carefully because the subtraction procedure may lead to artificial bands in the range of the photolysis bands. Therefore, an independent control is helpful to support or to question the attribution of difference bands to $Ca_2E_1 \rightarrow Ca_2E_1P$-bands. This is done by calculating $Ca_2E_1 \rightarrow Ca_2E_1P$-transient-spectra (see Experimental procedures section) shown in Fig. 3D. Bands which appear in both, the $Ca_2E_1 \rightarrow Ca_2E_1P$-spectra (Fig. 3C) and the respective transient-spectra (Fig. 3D), are attributed to the formation of Ca_2E_1P; they are termed $Ca_2E_1 \rightarrow Ca_2E_1P$-bands and listed in Table 3. Bands which are very weak in both spectra are attributed tentatively to $Ca_2E_1 \rightarrow Ca_2E_1P$-bands and marked with a question mark in Table 3. The tentative attribution of the bands at 1256, 1232 and 1162 cm^{-1} (see Fig. 3C) is justified by their appearance as shoulders in the transient-spectra (1256 and 1232 cm^{-1}, Fig. 3D) or in the flash-induced-spectra (1162 cm^{-1}, Fig. 3A).

$Ca_2E_1 \rightarrow Ca_2E_1P$-(high Ca^{2+})-samples contained in addition to the $Ca_2E_1 \rightarrow Ca_2E_1P$-samples 20 mM $CaCl_2$ and 0.5 mg/ml Ca^{2+}-ionophore A23187 to ensure equal distribution of Ca^{2+} inside and outside the vesicles. Because of the high Ca^{2+}-concentration, the activity of the samples was very low and the decay of $Ca_2E_1 \rightarrow Ca_2E_1P$-bands could not be observed. The

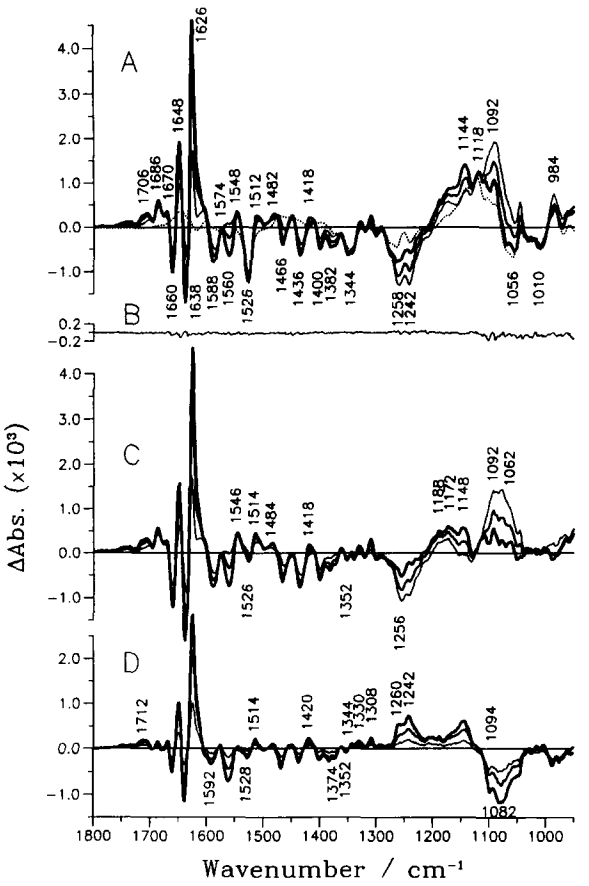

Fig. 4. IR difference spectra after ATP release in $Ca_2E_1 \rightarrow Ca_2E_1P$-samples in ^2H_2O. $T = 1°C$, average of three samples. The numbers give the band positions of the bold line spectra. (A) Full lines: flash-induced-spectra ΔA_x, bold: ΔA_1, medium: average of ΔA_2 and ΔA_3, thin: ΔA_5. Dotted line: Photolysis spectrum. (B) Baseline spectrum ΔA_b. (C) $Ca_2E_1 \rightarrow Ca_2E_1P$-spectra, calculated from bold: ΔA_1, medium: average of ΔA_2 and ΔA_3, thin: ΔA_5. (D) $Ca_2E_1 \rightarrow Ca_2E_1P$-transient-spectra: flash-induced-spectra ΔA_x minus ΔA_5, bold: ΔA_1, medium: ΔA_2, thin: ΔA_3.

$Ca_2E_1 \rightarrow Ca_2E_1P$-spectra of these samples (not shown) are in excellent agreement with those discussed above of the samples with low Ca^{2+} concentration with the following exceptions: The small broad band around 1750 cm^{-1} nearly disappears, the band at 1714 cm^{-1} shifts to 1720 cm^{-1}, and between 1592 and 1560 cm^{-1} negative bands are very small.

3.3. Formation of Ca_2E_1P from Ca_2E_1 in ^2H_2O

Fig. 4 shows the difference spectra of Ca_2E_1P formation in ^2H_2O (reaction step (2) in Fig. 1B). As in H_2O, the final spectrum taken 3.5 min after ATP release (thin line in Fig. 4A) resembles the spectrum of ADP-binding (Fig. 2C). Most bands clearly appear in both the $Ca_2E_1 \rightarrow Ca_2E_1P$-spectra (Fig. 4C) and the respective transient-spectra (Fig. 4D) and can therefore securely be attributed to the $Ca_2E_1 \rightarrow Ca_2E_1P$-bands. They are listed in Table 3. Other bands appearing in Fig. 4C can tentatively be attributed to these bands because they lead to a different shape or position of bands when the flash-induced-spectra are compared with the photolysis spectrum (broad band between 1200 and 1120 cm^{-1}, Fig. 4A) or appear in the transient-spectra (Fig. 4D) as a dip (1256 cm^{-1}), a positive band (1092 cm^{-1}) or a shoulder (1062 cm^{-1}). The positive band at 1546 cm^{-1} is not seen in the transient-spectra. As this band cannot be explained by the photolysis spectrum (dotted line in Fig. 4A), it must be attributed to the ATPase-nucleotide-complex, caused probably by nucleotide binding. This would explain its missing in transient-spectra, because in the final state at least part of the ATPase binds ADP. In fact, this band appears in the ADP-binding-spectra (Fig. 2C), making the attribution to nucleotide binding plausible.

Spectra of $Ca_2E_1 \rightarrow Ca_2E_1P$-(high Ca^{2+})-samples (not shown) in ^2H_2O showed the same bands as the $Ca_2E_1 \rightarrow Ca_2E_1P$-spectra, with the following exceptions: The small broad band around 1750 cm^{-1} narrows and the band with its maximum at 1706 cm^{-1} in the flash-induced-spectra appears at 1714 cm^{-1}.

3.4. Comparison of ADP-binding-spectra and $Ca_2E_1 \rightarrow Ca_2E_1P$-spectra

The bands observed in the $Ca_2E_1 \rightarrow Ca_2E_1P$-spectra (Figs. 3C and 4C) are due to the phosphorylation reaction, as well as to binding of ATP. The reason for this is that ATP binding is not only an intermediate step of the phosphorylation reaction, but also occurs to the phosphoenzyme, if ATP is released in excess. In order to distinguish between nucleotide-binding-bands and bands arising from the phosphorylation reaction (named phosphorylation bands), ADP-binding-spectra and $Ca_2E_1 \rightarrow Ca_2E_1P$-spectra were normalized (see Experimental procedures section) and are compared in Fig. 5. The difference between the ADP-binding- and the $Ca_2E_1 \rightarrow Ca_2E_1P$-spectrum reflects reaction step (3) in Fig. 1B, i.e., the exchange of ADP for ATP and the phosphorylation reaction. It is furtheron termed phosphorylation spectrum. Bands that can be attributed to ATPase phosphorylation and ADP/ATP-exchange are named phosphorylation bands and listed in Table 4. To count a band to the phosphorylation bands, the only fact that it appears in the phosphorylation spectra is not sufficient because artificial bands have to be considered arising from the subtraction procedures and the normalization. Thus, a phosphorylation band has to manifest itself also in a different shape or position of bands when comparing ADP-binding-spectra with $Ca_2E_1 \rightarrow Ca_2E_1P$-spectra. Bands which were not attributed to $Ca_2E_1 \rightarrow Ca_2E_1P$-bands or ADP-binding-bands in the preceding sections are not considered (for example the 1470 cm^{-1} band in

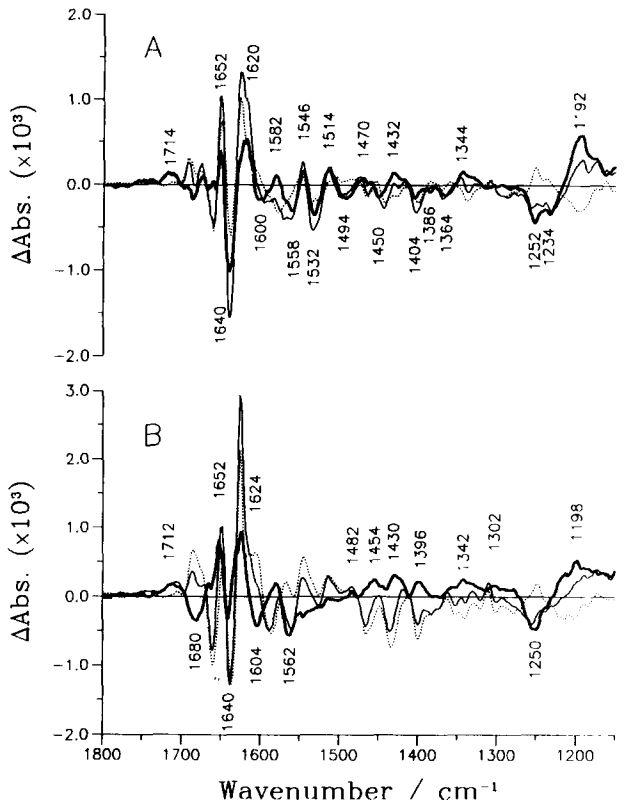

Fig. 5. Normalized IR difference spectra associated with ATPase phosphorylation. $T = 1°C$. The numbers give the band positions of the bold line spectra. (A) Difference spectra in H_2O. Bold line: phosphorylation spectrum (normalized $Ca_2E_1 \rightarrow Ca_2E_1P$-spectrum minus normalized ADP-binding-spectrum). Thin line: normalized $Ca_2E_1 \rightarrow Ca_2E_1P$-spectrum, average of two samples, calculated from ΔA_1. Dotted line: normalized ADP-binding-spectrum, calculated from the average of ΔA_2 to ΔA_4 of four samples. (B) Difference spectra in ^2H_2O. Bold line: phosphorylation spectrum (normalized $Ca_2E_1 \rightarrow Ca_2E_1P$-spectrum minus normalized ADP-binding-spectrum). Thin line: normalized $Ca_2E_1 \rightarrow Ca_2E_1P$-spectrum, calculated from the average of ΔA_1 and ΔA_2 of three samples. Dotted line: normalized ADP-binding-spectrum, calculated from the average of ΔA_1 to ΔA_4 of two samples.

Table 4
Phosphorylation bands arising from ATPase phosphorylation and exchange of ADP for ATP

H_2O	D_2O	H_2O	D_2O
1714 (+)	1712 (+)	1514 (+)	
	1680 (−)	1494 (−)	1482 (+)
1652 (+)(?)	1652 (+)(?)	1450 (−)	1454 (+)
1640 (−)	1640 (−)(?)	1432 (+)	1430 (+)
1620 (+)	1624 (+)	1404 (−)	1396 (+)
1600 (−)	1604 (−)	1386 (−)	
1582 (+)(?)	1580 (+)	1364 (−)	
1558 (−)	1562 (−)	1344 (+)(?)	
1546 (+)		1252 (−)(?)	1250 (−)(?)
1532 (−)(?)		1234 (−)(?)	

The numbers give the positions of the difference bands in wavenumbers. (?) means that the attribution is not secure, (+) or (−) mean positive or negative band.

Fig. 5A). Using this general procedure, only the band at 1532 cm^{-1} remains to be discussed. It is clearly present in the $Ca_2E_1 \rightarrow Ca_2E_1P$-spectra and the respective transient-spectra in H_2O. However, it is not clear whether this band is already present in the ADP-binding-spectra, since it is in the region of a photolysis band and may appear too small in the ADP-binding-spectra, if the photolysis spectrum is not normalized correctly before subtraction.

Many bands of the $Ca_2E_1 \rightarrow Ca_2E_1P$-spectra arise from nucleotide binding: For samples in H_2O (Fig. 5A, the positions of the bands are labelled in Fig. 3) the bands at 1692, 1676, 1660, 1650, 1464, 1444, 1402 and at 1368 cm^{-1}, as well as parts of the bands at 1638 and 1626 cm^{-1}; for samples in ^2H_2O (Fig. 5B, the band positions are labelled in Fig. 4) the bands at 1686, 1670, 1660, 1648, 1638, 1588, 1514, the bands between 1500 an 1300 cm^{-1} and part of the 1626 cm^{-1} band. Differences between the $Ca_2E_1 \rightarrow Ca_2E_1P$-spectrum and the ADP-binding-spectrum around 1650 cm^{-1} are probably due to variations between the individual samples. Below 1150 cm^{-1}, no differences between ADP-binding-spectrum and $Ca_2E_1 \rightarrow Ca_2E_1P$-spectrum can reliably be detected for reason of strong overlap by photolysis bands.

3.5. Formation of E_2P from Ca_2E_1 in H_2O

$Ca_2E_1 \rightarrow E_2P$-samples were prepared without Na^+ and K^+, but with 15 mM Mg^{2+}. They contained the Ca^{2+}-ionophore A23187 in order to prevent a high Ca^{2+}-concentration inside the vesicles. It can be assumed that the ADP-insensitive phosphoenzyme (E_2P) accumulates in these samples (see discussion section). Fig. 6 shows the difference spectra of these samples induced by ATP release in H_2O reflecting reaction step (4) in Fig. 1B. Bands that appear in $Ca_2E_1 \rightarrow E_2P$-spectra and in the respective transient-spectra are counted to $Ca_2E_1 \rightarrow E_2P$-bands and listed in Table 5. Small bands are tentatively assigned to these bands. In the region from 1450 to 1370 cm^{-1}, the transient-spectra (Fig. 6D) show the same difference signal like the $Ca_2E_1 \rightarrow E_2P$-spectra (Fig. 6C) but vertically shifted to higher ΔA values. Because on one hand the $Ca_2E_1 \rightarrow E_2P$-spectra are sensitive to subtraction of the photolysis spectrum, and on the other hand the transient-spectra do not show baseline instabilities, we think that the transient-spectra are more reliable for the attribution of bands in this region (positive bands at 1434 and 1396 cm^{-1}). The flash-induced-spectra in the region of the photolysis bands between 1290 and 1200 cm^{-1} show a complicated structure with 4 negative bands at 1268, 1256, 1244 and 1234 cm^{-1}. The 1268 and 1234 cm^{-1} bands coincide with photolysis bands, which seem to be incompletely subtracted in the $Ca_2E_1 \rightarrow E_2P$-spectra (Fig. 6C). By multiplication of the photolysis spectrum

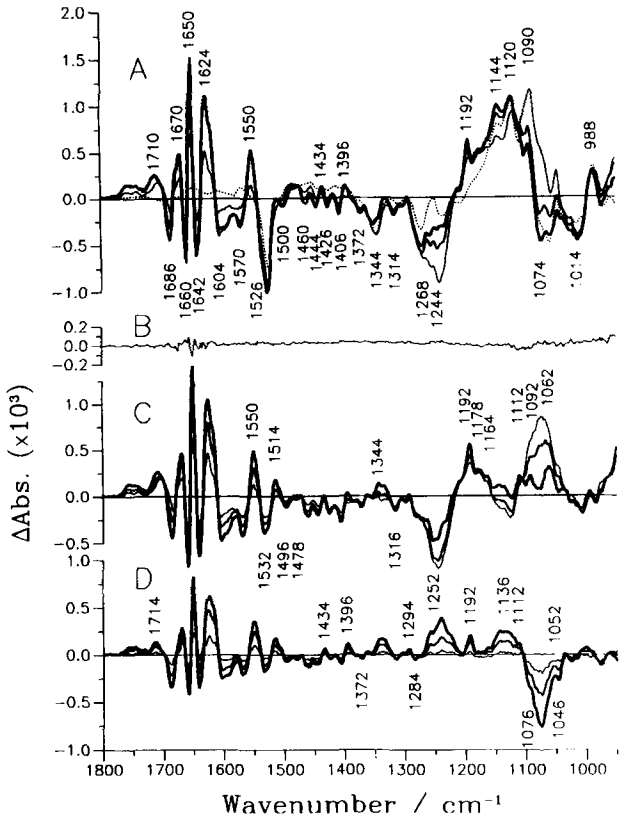

Fig. 6. IR difference spectra after ATP release in $Ca_2E_1 \rightarrow E_2P$-samples in H_2O. $T = 1°C$, average of seven samples. The numbers give the band positions of the bold line spectra. (A) Full lines: flash-induced-spectra ΔA_x, bold: ΔA_1, medium: ΔA_2, thin: ΔA_6. Dotted line: Photolysis spectrum. (B) Baseline spectrum ΔA_b. (C) $Ca_2E_1 \rightarrow E_2P$-spectra calculated from bold: ΔA_1, medium: average of ΔA_2 and ΔA_3, thin: average of ΔA_5 and ΔA_6. (D) $Ca_2E_1 \rightarrow E_2P$-transient-spectra: flash-induced-spectra ΔA_x minus average of ΔA_5 and ΔA_6, bold: ΔA_2, medium: ΔA_3, thin: ΔA_4.

by an appropriate constant and recalculation of the $Ca_2E_1 \rightarrow E_2P$-spectra, only two negative bands appear in this region at 1284 and 1252 cm^{-1}. Both show up as negative band or as indention in the transient-spectra (Fig. 6D). However, we are careful in attributing them to $Ca_2E_1 \rightarrow E_2P$-bands, since in this spectral region the photolysis bands are sensitive to buffer composition.

$Ca_2E_1 \rightarrow E_2P$-(+Me_2SO)-samples contained 20% Me_2SO in addition to the $Ca_2E_1 \rightarrow E_2P$-samples. The activity of these samples in H_2O was too low to observe the decay of the $Ca_2E_1 \rightarrow E_2P$-bands within the time of the experiment (4 min). The addition of Me_2SO leads to few changes in the $Ca_2E_1 \rightarrow E_2P$-spectra (data not shown): The 1710 cm^{-1} band shifts to 1708 cm^{-1}, the 1642 cm^{-1} band shows reduced intensity and the positive 1514 cm^{-1} band disapears. The 1112 cm^{-1} and the 1062 cm^{-1} band are clearly seen already in the flash-induced-spectra as shoulder or as positive band.

3.6. Formation of E_2P from Ca_2E_1 in ^2H_2O

Fig. 7 shows the difference spectra of the $Ca_2E_1 \rightarrow E_2P$-(+Me_2SO)-samples in ^2H_2O reflecting reaction step (4) in Fig. 1B. In contrast to the respective samples in H_2O, the decay of the $Ca_2E_1 \rightarrow E_2P$-bands could be observed in ^2H_2O suggesting that the released ATP is consumed within the time of the experiment, and therefore a higher activity of these samples in ^2H_2O as compared to H_2O. Bands that appear in the $Ca_2E_1 \rightarrow E_2P$-(+Me_2SO)-spectra and the respective transient-spectra (Figs. 7C and D) are listed in Table 5 as $Ca_2E_1 \rightarrow E_2P$-bands. The 1436 cm^{-1} band is not present in the transient-spectra (Fig. 7D), but shows up very clearly in the flash-induced-spectra (full lines in Fig. 7A) and is therefore counted to the $Ca_2E_1 \rightarrow E_2P$-bands.

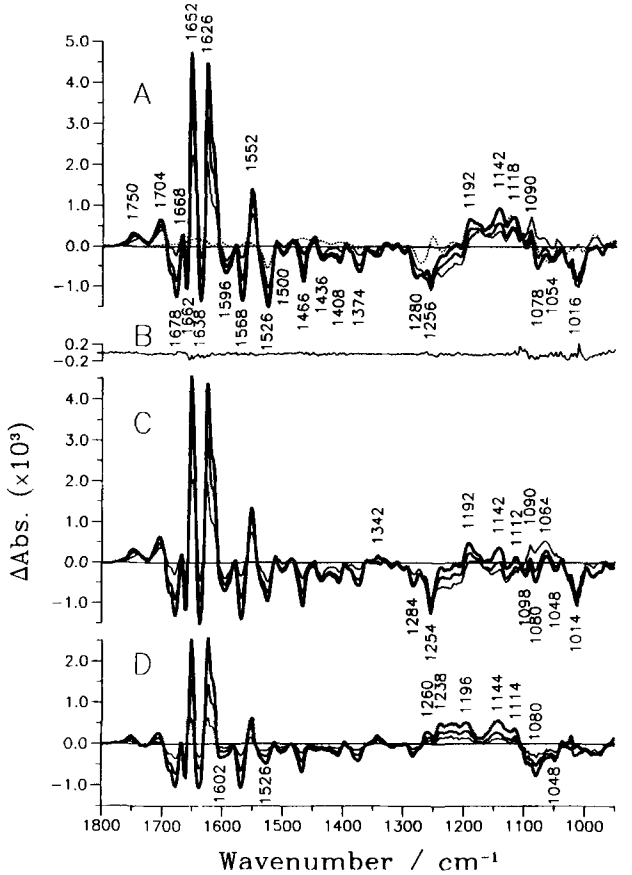

Fig. 7. IR difference spectra after ATP release in $Ca_2E_1 \rightarrow E_2P$-(+Me_2SO)-samples in ^2H_2O. $T = 1°C$, average of two samples. The numbers give the band positions of the bold line spectra. (A) Full lines: flash-induced-spectra ΔA_x, bold: average of ΔA_1 to ΔA_3, medium: average of ΔA_4 and ΔA_5, thin: flash-induced-spectrum recorded 7 min after the photolysis flash. Dotted line: Photolysis spectrum. (B) Baseline spectrum ΔA_b. (C) $Ca_2E_1 \rightarrow E_2P$-spectra, calculated from bold: average of ΔA_1 to ΔA_3, medium: ΔA_5, thin: ΔA recorded 7 min after the photolysis flash. (D) $Ca_2E_1 \rightarrow E_2P$-transient-spectra: flash-induced-spectra ΔA_x minus flash-induced-spectrum recorded 7 min after the photolysis flash, bold: average of ΔA_1 to ΔA_3, medium: average of ΔA_4 and ΔA_5, thin: ΔA_7.

When Me_2SO is omitted from these samples the spectra showed features intermediate between the $Ca_2E_1 \rightarrow Ca_2E_1P$-spectra and the $Ca_2E_1 \rightarrow E_2P$-($+Me_2SO$)-spectra (Fig. 7), but resembled more the $Ca_2E_1 \rightarrow Ca_2E_1P$-spectra (data not shown). This is in contrast to the $Ca_2E_1 \rightarrow E_2P$-samples in H_2O where the addition of Me_2SO only lead to few changes in the spectrum.

3.7. Comparison between $Ca_2E_1 \rightarrow Ca_2E_1P$-spectra and $Ca_2E_1 \rightarrow E_2P$-spectra

In order to calculate a difference spectrum for the phosphoenzyme conversion from Ca_2E_1P to E_2P (step (5) in Fig. 1B), $Ca_2E_1 \rightarrow Ca_2E_1P$-spectra and $Ca_2E_1 \rightarrow E_2P$-spectra were normalized to the same protein content and are shown in Fig. 8 in H_2O and ^2H_2O (Figs. 8A and B, respectively). The difference, termed $Ca_2E_1P \rightarrow E_2P$-spectrum, is shown as bold line. Table 6 lists the position of those bands of the $Ca_2E_1P \rightarrow E_2P$-spectrum which are connected with phosphoenzyme conversion and Ca^{2+}-release. They are named $Ca_2E_1P \rightarrow E_2P$-bands. As already discussed for the phosphorylation bands, the appearance of a band in the $Ca_2E_1P \rightarrow E_2P$-spectra is not sufficient to count it to the $Ca_2E_1P \rightarrow E_2P$-bands. It has to reveal itself in a different position or shape of a band when comparing the $Ca_2E_1 \rightarrow Ca_2E_1P$-spectrum and the $Ca_2E_1 \rightarrow E_2P$-spectrum as well as the respective transient-spectra. Some bands can only be tentatively attributed to $Ca_2E_1P \rightarrow E_2P$-bands because they are superimposed by photolysis bands or are in the region of the strongest protein and water absorption, where band intensities of different samples showed strong variations. With the exception of the 1192 cm^{-1} band, no absorbance changes below 1200 cm^{-1} can be attributed safely to the $Ca_2E_1P \rightarrow E_2P$ conversion because they are masked by the strong photolysis bands.

Table 5
$Ca_2E_1 \rightarrow E_2P$-bands of the $Ca_2E_1 \rightarrow E_2P$-samples in H_2O and the $Ca_2E_1 \rightarrow E_2P$-($+Me_2SO$)-samples in ^2H_2O

H_2O	D_2O	H_2O	D_2O
1750 (+)	1750 (+)	1426 (−)	
1710 (+)	1704 (+)	1406 (−)	1408 (−)
1686 (−)	1678 (−)	1396 (+)	
1670 (+)		1372 (−)	1374 (−)
1660 (−)	1662 (−)	1344 (+)	1342 (+)
1650 (+)	1652 (+)	1316 (−)(?)	
1642 (−)	1638 (−)	1294 (+)(?)	
1624 (+)	1626 (+)	1284 (−)(?)	1284 (−)
1604 (−)	1596 (−)	1252 (−)(?)	1254 (−)
1570 (−)	1568 (−)	1192 (+)	1192 (+)
1550 (+)	1552 (+)	1178 (+)(?)	
1532 (−)	1526 (−)	1164 (+)(?)	
1514 (+)	1500 (−)	1144 (+)(?)	1142 (+)
1496 (−)		1112 (+)(?)	1112 (+)(?)
1478 (−)		1092 (+)(?)	1098 (−)(?)
1460 (−)	1466 (−)		1080 (−)(?)
1444 (−)		1062 (+)(?)	1064 (+)(?)
1434 (+)	1436 (−)		1048 (−)(?)

The numbers give the positions of the difference bands in wavenumbers. (?) means that the attribution is not secure, (+) or (−) mean positive or negative band.

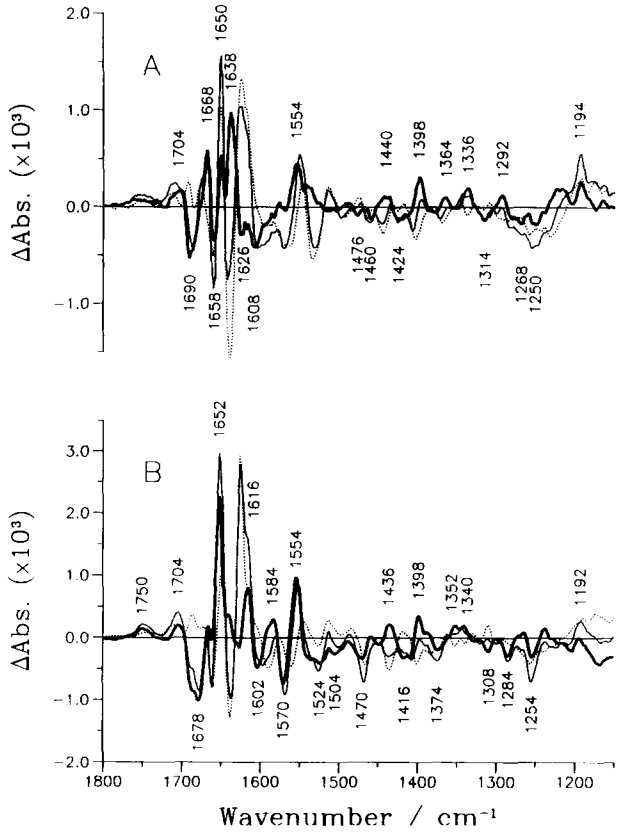

Fig. 8. Normalized IR difference spectra associated with $Ca_2E_1P \rightarrow E_2P$ conversion and Ca^{2+}-release. $T = 1°C$. The numbers give the band positions of the bold line spectra. (A) Difference spectra in H_2O. Bold line: $Ca_2E_1P \rightarrow E_2P$-spectrum (normalized $Ca_2E_1 \rightarrow E_2P$-spectrum minus normalized $Ca_2E_1 \rightarrow Ca_2E_1P$-spectrum). Thin line: normalized $Ca_2E_1 \rightarrow E_2P$-spectrum, calculated from the average of ΔA_1 and ΔA_2 of four samples. Dotted line: normalized $Ca_2E_1 \rightarrow Ca_2E_1P$-spectrum, calculated from ΔA_2, average of two samples. (B) Difference spectra in ^2H_2O. Bold line: $Ca_2E_1P \rightarrow E_2P$-spectrum (normalized $Ca_2E_1 \rightarrow E_2P$-($+Me_2SO$)-spectrum minus normalized $Ca_2E_1 \rightarrow Ca_2E_1P$-spectrum). Thin line: normalized $Ca_2E_1 \rightarrow E_2P$-($+Me_2SO$)-spectrum, calculated from the average of ΔA_2 and ΔA_3 of two samples. Dotted line: normalized $Ca_2E_1 \rightarrow Ca_2E_1P$-spectrum, calculated from the average of ΔA_1 and ΔA_2 of three samples.

4. Discussion

4.1. FTIR difference spectra

Starting from Ca_2E_1, three steps of the ATPase reaction cycle were investigated with IR difference spectroscopy in H_2O and ^2H_2O: (a) nucleotide- (ADP-)

Table 6
$Ca_2E_1P \rightarrow E_2P$-bands arising from phosphoenzyme conversion and Ca^{2+}-release

H_2O	D_2O	H_2O	D_2O
1756 (+)	1750 (+)		1504 (−)
1704 (+)	1704 (+)	1476 (−)	1470 (−)
1690 (−)	1678 (−)	1460 (−)	
1668 (+)		1440 (+)(?)	1436 (+)
1658 (−)(?)		1424 (−)	1416 (−)
1650 (+)(?)	1652 (+)	1398 (+)	1398 (+)
1638 (+)		1364 (+)	1374 (−)
1626 (−)	1616 (+)		1352 (+)(?)
1608 (−)	1602 (−)	1336 (+)	1340 (+)(?)
	1584 (+)	1314 (−)(?)	1308 (−)
	1570 (−)	1292 (+)(?)	1284 (−)
1554 (+)	1554 (+)		1254 (−)
	1524 (−)	1192 (+)	1192 (+)

The numbers give the positions of the difference bands in wavenumbers. (?) means that the attribution is not secure, (+) or (−) mean positive or negative band.

binding (step (1) in Fig. 1B), (b) formation of Ca_2E_1P (step (2) in Fig. 1B) and (c) formation of E_2P (step (4) in Fig. 1B).

Photolytic release of ATP or ADP from their caged analogues was used to start the reaction in the IR cuvette. From the spectra before and after the release, IR difference spectra could be calculated directly. These flash-induced-spectra contain absorbance changes due to the photolysis reaction, hydrolysis of ATP and structural changes in the protein-nucleotide complex. The latter kind of absorbance change could be separated from the first by subtracting a difference spectrum of the photolysis reaction from the flash-induced-spectra. In this way photolysis bands cancel and the obtained spectra are named according to the reaction investigated (see Table 1b and Experimental procedures section). ATP-hydrolysis gives rise to absorbance changes in the spectra of phosphoenzyme formation. However, in the spectrum recorded immediately after release of ATP, hydrolysis bands had developed to only a small extent because of the short time between ATP release and recording of the spectra. For this reason, this spectrum (bold line in Figs. 3C, 4C, 6C and 7C) and the ADP-binding-spectra (thin line in Figs. 2A and C) show absorbance changes mainly arising from structural changes of the protein polypeptide backbone, of amino acid side chains and of the nucleotide upon its binding to the ATPase.

Suspension of the ATPase in ^2H_2O results in deuteration of acidic groups (OH, SH, NH_x), and therefore may lead to shifts of IR band positions. However, only part of the ATPase is accessible for the solvent ^2H_2O, and therefore not all acidic groups are deuterated [7].

4.2. Accumulation of Ca_2E_1P or E_2P in our samples

After addition of ATP to Ca_2E_1 under optimal conditions, the ATPase is phosphorylated to an extent of nearly 100% until all ATP is consumed. K^+ activates hydrolysis of the ADP-insensitive phosphoenzyme (E_2P). In the presence of 100 mM K^+, the phosphoenzyme conversion from Ca_2E_1P to E_2P is therefore the rate-limiting step, and 75–90% of the ATPases are in the ADP-sensitive form (Ca_2E_1P) [8–10]. However, due to the high ATPase concentration of 1 mM in our IR-samples the concentration of the reaction product ADP is also in the millimolar range, which may lead to a decrease in the amount of phosphoenzyme. Pickart and Jencks [11] reported 40% phosphoenzyme in the presence of millimolar concentrations of ADP and ATP, but at a 100 times lower ATPase concentration. In order to test the effect of ADP on our $Ca_2E_1 \rightarrow Ca_2E_1P$-spectra, we removed it by adding 2 μg adenylate kinase to $Ca_2E_1 \rightarrow Ca_2E_1P$-samples. The resulting difference spectra were in perfect agreement with those lacking adenylate kinase, with the exception of 2 difference bands which are diagnostic for the consumption of ADP (at 930 cm^{-1}) and for the production of AMP (at 984 cm^{-1}) by adenylate kinase. We thus assume that the Ca_2E_1P intermediate accumulates in our K^+-containing samples ($Ca_2E_1 \rightarrow Ca_2E_1P$-samples).

High Ca^{2+} concentrations (> 1 mM) inhibit ATPase activity [12,13], presumably due to binding of Ca^{2+} to the luminal low affinity Ca^{2+} binding sites. In the presence of high Ca^{2+} concentrations, the phosphoenzyme is nearly exclusively in the Ca_2E_1P form [14,15], but part of the ATPase is unphosphorylated and binds Ca · ATP, which phosphorylates the ATPase 10 times slower than Mg · ATP [16]. The addition of Ca^{2+} at high concentrations ($Ca_2E_1 \rightarrow Ca_2E_1P$-(high Ca^{2+})-samples) leads to only very small changes in the difference spectra (see Results section), indicating again that the Ca_2E_1P intermediate accumulated in both the $Ca_2E_1 \rightarrow Ca_2E_1P$-samples and the $Ca_2E_1 \rightarrow Ca_2E_1P$-(high Ca^{2+})-samples in H_2O and ^2H_2O.

In buffers where K^+ is omitted or replaced by Li^+, with high Mg^{2+}- (~ 10 mM) and low Ca^{2+}-concentrations (< 100 μM), hydrolysis of E_2P is the rate limiting step of the reaction cycle and E_2P accumulates to 70–100% [8,9,15]. The amount of E_2P can be enhanced by the addition of Me_2SO [8], since Me_2SO shifts the equilibrium of E_2P hydrolysis towards the phosphoenzyme [17]. In H_2O, the difference spectra of the K^+-free samples with and without 20% Me_2SO ($Ca_2E_1 \rightarrow E_2P$-samples and $Ca_2E_1 \rightarrow E_2P$-(+Me_2SO)-samples) were nearly identical (see Results section). We therefore conclude that in H_2O E_2P accumulates in both kinds of samples. However, when ^2H_2O was used as solvent, the addition of Me_2SO led

to significant changes in the difference spectrum. Without Me_2SO the characteristic bands of the $Ca_2E_1 \rightarrow E_2P$-(+Me_2SO)-spectrum are observed only to a small extent and the difference spectrum resembled more the $Ca_2E_1 \rightarrow Ca_2E_1P$-spectra than the $Ca_2E_1 \rightarrow E_2P$-(+Me_2SO)-spectra. We conclude that in ^2H_2O E_2P accumulates only in the Me_2SO-containing samples ($Ca_2E_1 \rightarrow E_2P$-(+Me_2SO)-samples). Because of the high concentration of released ATP, we can assume that in our samples ATP is bound to every phosphoenzyme intermediate [1,18–20].

4.3. Isotope effect of ^2H_2O on E_2P-hydrolysis

As mentioned above, E_2P accumulates to a lower amount in ^2H_2O than in H_2O in Me_2SO-free samples. This may have two reasons: The $Ca_2E_1P \rightarrow E_2P$ conversion may be inhibited in ^2H_2O, or E_2P hydrolysis may be activated. The last hypothesis is supported by the significantly higher activity of Me_2SO-containing samples in ^2H_2O as compared to H_2O (see Results section). This increase of a reaction rate in ^2H_2O represents an inverse kinetic isotope effect which is observed for acid-catalyzed reactions, if the reaction steps following the initial protonation step are rate limiting [21,22]. The effect is due to the weaker acidity and therefore higher concentration of the protonated intermediate in ^2H_2O.

4.4. Band assignment for the ADP-binding-spectra in H_2O and ^2H_2O

ADP-binding-spectra in H_2O and ^2H_2O are shown in Fig. 2 reflecting reaction step (1) in Fig. 1B. The large number of difference bands observed complicates an unambiguous assignment to functional groups by simply considering the vibrational frequency. Instead, we shall propose tentative assignments on the basis of the frequency region, relative intensities and deuteration effects, in general based on [23], on [24,25] for amino acid side chains, on [26–30] for amide I absorption and on [31] for adenosine absorption.

ADP-binding leads to absorbance changes which are comparable in number and magnitude with those of phosphoenzyme formation (Fig. 5, step (2) in Fig. 1B) indicating that the extent of structural changes is roughly the same in both steps. In the region between 1700 and 1620 cm^{-1}, the amide I mode of the peptide group absorbs, as well as amino acid side chain groups and the adenine base (1650 cm^{-1}). The bands around 1685 cm^{-1} can be assigned to strongly hydrogen bonded carboxyl groups ($\nu_{C=O}$ of Asp and Glu), or alternatively to the amide I vibration (peptide $\nu_{C=O}$) of β-sheet or β-turn structure. Both functional groups absorb in ^2H_2O at about 10 cm^{-1} lower wavenumbers [24,25,27,30], a fact which is also observed in our spectra. These bands around 1685 cm^{-1} are stronger in ^2H_2O (compare dotted lines in Figs. 5A and B). This may be due to the superposition of a negative band in H_2O shifting to lower wavenumbers in ^2H_2O. Such a band may be assigned to the $\nu_{C=O}$ of Asn or Gln, absorbing around 1680 cm^{-1} in H_2O and shifting to 1650 cm^{-1} (Asn) or 1635 cm^{-1} (Gln) in ^2H_2O, where it may contribute to the negative bands which are stronger in ^2H_2O than in H_2O.

Changes in protein conformation which lead to a variation in the amide I absorption are the most probable explanation for the bands at 1660, 1650 and 1638 cm^{-1} in H_2O and ^2H_2O. These signals may be interpreted in terms of a local decrease of the amount of β-sheet and coil structure with concominant increase for α-helical structure, but an alternative interpretation is a decrease in linewidth of an α-helical structure leading to a positive band with negative side lobes. The reason may be a reduction in heterogeneity or motional freedom. In addition to contributions from peptide C = O groups, we have to consider IR signals arising from vibrations of amino acid side chain groups such as His, Arg, Asn or Gln. However, the NH_2^+ mode of His is an unlikely candidate because of its small extinction coefficient. Contributions of Arg modes and the δNH_2^+ mode of Asn and Gln are improbable, since the typical band shifts upon deuteration are not observed. Most bands are stronger in ^2H_2O, possibly a consequence of a shift of some of them resulting in a better separation of positive and negative bands.

The positive 1626 cm^{-1} band is composed of several signals, in H_2O as well as in ^2H_2O. The maximum as well as the shoulders gain intensity in ^2H_2O. This band is in the range of the amide I mode of β-sheet structures, but also at the high-frequency edge of the antisymmetric stretch vibration of carboxylates ($\nu_{as}(COO^-)$). In ^2H_2O, a weak His band or a Tyr ring vibration may contribute to the 1626 cm^{-1} band, too. The latter absorbs in H_2O solution at approx. 1600 cm^{-1} and thus may hide the negative band that appears in the ADP-binding-spectra in ^2H_2O at 1586 cm^{-1}. A contribution from amine groups of exchangeable amino acid side chains or adenine to the 1626 cm^{-1} band is unlikely, since the typical band shifts in ^2H_2O to approx. 1230 cm^{-1} [32] or 1190 cm^{-1}, respectively, were not observed.

Asp and Glu carboxylate groups ($\nu_{as}(COO^-)$) in aqueous solution absorb between 1580 and 1560 cm^{-1} (in ^2H_2O upshifted by 10 cm^{-1}) at positions which are also found for an adenine ring vibration. The amide II mode of the peptide group absorbs around 1550 cm^{-1}. In this region, no clear ADP-binding-bands are observed in H_2O. In contrast, two positive bands at 1566 and 1546 cm^{-1} are observed in ^2H_2O. These bands can be assigned to either COO^- or Trp modes or to amide II modes not accessible for deuteration. As the

two bands are not observed in H_2O, we postulate a negative amide II band superimposed upon them in ^2H_2O, but shifting to 1466 cm^- in ^2H_2O, where it contributes to the strong negative band. The 1514 cm^{-1} band in ^2H_2O may be assigned to a Tyr ring mode. However, the reason for its absence in H_2O is unclear, since only a slight upshift by ca. 4 cm^{-1} would be expected.

Carboxylate salts absorb in the region of 1470–1400 cm^{-1} ($\nu_s(COO^-)$) dependant on the structure of the metal-carboxylate complex [33]. Other groups absorb at better defined wavenumbers in this region: CH_3- and CH_2-groups, Trp and the amide II mode in ^2H_2O around 1466 cm^{-1}, proline around 1454 and 1420 cm^- [34,35]. The negative bands at 1444 and 1428 cm^{-1} in H_2O merge to one band at 1432 cm^{-1} in ^2H_2O. This may be caused by opposite shifts of the two bands consequent to deuteration. For example, an adenine band absorbing at 1423 cm^{-1} shifts 2 cm^{-1} to higher wavenumbers. Its position depends upon the formation of hydrogen bonds [31]. In the region from 1450 to 1400 cm^{-1}, CH_2-groups with a neighboring carbonyl group, i.e., from Asp, Glu, Asn and Gln, also absorb. The indole ring of Trp absorbs at 1420 cm^{-1} and Tyr or carboxylate groups ($\nu_s(COO^-)$) of Glu or Asp in the aqueous phase may contribute at 1400 cm^{-1}.

Bands between 1400 and 1300 cm^{-1} can be tentatively assigned to either CH_3-groups (δ_s, 1370 cm^-) or adenine ring vibrations sensitive to hydrogen bonding (1370, 1340–1300 cm^{-1}) or Trp-modes (1350 cm^{-1}) or to CH-groups (1350–1315 cm^-).

Binding of phosphate groups to the ATPase is the most probable explanation for the bands below 1270 cm^{-1}. Dehydration of phosphate groups is best seen by an 20 cm^{-1} upshift of the $>PO_2^-$ stretch vibration [36,37], which absorbs at 1228 cm^{-1} in ATP and at 1208 cm^{-1} in ADP [2,3]. Indeed, in the ADP-binding-spectra, a negative band at 1192 cm^{-1} and a positive band at approx. 1240 cm^- are observed, as expected for an upshift of the $>PO_2^-$ band. However, contributions from Trp, Tyr and Phe cannot be excluded, since substituted benzenes also absorb between 1200 and 1000 cm^-.

4.5. Interpretation of the ADP-binding-spectra

The ADP-binding-spectra give several hints on the interaction between nucleotide and ATPase. The α-phosphate seems to become dehydrated and changes in hydrogen bonding to the nitrogen atoms of adenine cannot be excluded. In contrast, hydrogen bonding to the adenine NH_2-group apparently remains unchanged. In the case of the Na^+/K^+-ATPase, hydrogen bonds are observed to the adenine nitrogen atoms as well as to the NH_2-group [38].

Difference bands in the region of the amide I absorption of the peptide group strongly suggest the involvement of an α-helix in nucleotide binding, which is a common motiv for other nucleotide binding proteins because of the large dipole moment of an α-helix [39]. A modification of a β-sheet or turn structure is also likely to occur, in accordance with the proposition of Taylor and Green [40], who place the bound nucleotide at the C-terminus of a parallel β-sheet. We did not find hints for the participation of positively charged amino acid side chains in binding of the negatively charged phosphates. Lys does not seem to be involved in binding, since we did not find band shifts arising from the deuteration of the amine group. In the region of Arg absorption, bands in H_2O and ^2H_2O were found, but the typical band shifts of 50–60 cm^{-1} upon deuteration were not observed. However, this may be due to the overlap by other bands. The amino acid His is likely to participate in nucleotide binding because of the pH-dependency of ADP-binding [41], but is difficult to detect in IR spectroscopy because of the small extinction coefficient of its δNH_2^+ vibration.

Several difference bands were found that can tentatively be assigned to carboxylate groups of Asp and Glu. A modification of the Ca^{2+} binding site may be responsible for this since it is known that ATP and ADP accelerate Ca^{2+} binding [42,43].

4.6. Band assignment for the phosphorylation spectra in H_2O and ^2H_2O

The bold lines in Fig. 5 show the difference between the ADP-binding-spectra and the $Ca_2E_1 \rightarrow Ca_2E_1P$-spectra, i.e., the absorbance difference between $Ca_2E_1 \cdot ADP$ and $Ca_2E_1 \cdot ATP$ reflecting step (3) in Fig. 1B. For a detailed band assignment the reader is referred to the preceding discussion of the ADP-binding-spectra. However, some bands will be discussed here: The positive band around 1714 cm^{-1} can be assigned to C = O groups of Asp or Glu. If we assume that these C = O groups are newly formed from carboxylate groups via protonation or esterification, it can be estimated from the magnitude of the band that only one amino acid per ATPase is involved (based on the ϵ of the C = O group [24,25] and the amount of ATPase measured by amide I and amide II absorption, see Experimental procedures).

In the region of 1660–1620 cm^{-1}, peak positions in H_2O and ^2H_2O are nearly identical, indicating that amino acid side chains that are accessible to deuteration do not give a large contribution to the signals. The unchanged peak positions rather favor an assignment to peptide groups or to amino acid side chains in the core of the protein inaccessible for ^2H_2O.

The band at 1532 cm^{-1} in H_2O is not observed in ^2H_2O. This supports an assignment to the amide II mode of the peptide group. However, it is not clear

whether this band can be attributed to the phosphorylation bands (see Results section). A band which presumably corresponds to it in ^2H_2O at 1466 cm^{-1} is already present in the ADP-binding-spectra and does not change upon phosphorylation.

4.7. Interpretation of the phosphorylation spectra

Several processes happen upon phosphorylation of the ATPase from $Ca_2E_1 \cdot ATP$ to $Ca_2E_1P \cdot ATP$. (i) The residue Asp^{351} is phosphorylated, (ii) the two Ca^{2+} bound to the high affinity binding sites are occluded [1], and (iii) ADP is released [44]. (iv) A regulatory ATP binds at the catalytic site or is already bound to a different site [1,20,45,46]. Because the phosphorylation spectra are calculated from the difference between ADP-binding-spectra and $Ca_2E_1 \rightarrow Ca_2E_1P$-spectra, they also show the effects of ADP/ATP exchange.

Phosphorylation of Asp^{351} from ATP leads to chemical modifications of groups participating in the reaction which manifest themselves in the FTIR difference spectra. If the carboxylate group of Asp^{351} does not exhibit specific interactions with other amino acids, the two oxygen atoms equally share the negative charge. This resonance-stabilized COO^--form is abolished by phosphorylation, and a C = O and a C-O-P group originate. The corresponding absorbance bands at approx. 1580 cm^{-1} ($\nu_{as}(COO^-)$) and 1400 cm^{-1} ($\nu_s(COO^-)$) should show up as negative bands in the $Ca_2E_1 \rightarrow Ca_2E_1P$-spectra and the phosphorylation spectra and as positive bands at 1715 cm^{-1} ($\nu_{C=O}$), around 1270 cm^{-1} ($\nu_{C\text{-}O}$) and between 1030 and 900 cm^{-1} ($\nu_{O\text{-}P}$).

Concerning the absorption of the CO-O-P group, it can be expected that the bond order of the C-O bond rises due to resonance with the C = O group. This will lead to absorption at higher wavenumbers as compared to a C-O-P bond where the C-atom is part of an aliphatic moiety (absorption at 1030 cm^{-1} [23,47]). A similar effect is observed for the C-O-C group: The C-O absorbance shifts at most 200 cm^{-1} to higher wavenumbers if one C-atom is part of a phenyl ring or an ester group. We thus assume that the absorption of the CO-O-P group is better modelled by the aromatic rather than the aliphatic C-O-P connection which absorbs between 1260 and 1160 cm^{-1}. This conclusion is supported by the absorption of the K^+/Li^+ salt of acetyl phosphate in aqueous solution (data not shown) with bands at 1270 ($\nu_{C\text{-}O}$), 1128 ($\nu_{as}(\text{-}PO_3^{2-})$), 982 ($\nu_s(\text{-}PO_3^{2-})$) and 936 cm^{-1} ($\nu_{P\text{-}O}$).

Phosphorylation modifies phosphate groups in a similar way as does hydrolysis. A $> PO_2^-$ group disappears and a $\text{-}PO_3^{2-}$ group appears with corresponding positive bands at 1170 and 1080 cm^{-1} and a negative band at 1230 [2,3].

Some of these expected difference bands appear in the $Ca_2E_1 \rightarrow Ca_2E_1P$-spectra. At 1714 cm^{-1}, a carbonyl band is observed which we tentatively attribute to the phosphorylation site Asp^{351}. The negative bands in the 1600–1560 cm^{-1} and 1450–1400 cm^{-1} regions may indicate the disappearing COO^- group. However, these bands appear already upon ADP-binding, indicating that ADP-binding is sufficient to abolish the resonance isomery of the carboxyl group. On the other hand, it is possible that the ATPase in the Ca_2E_1 state develops specific interactions to the Asp^{351} carboxyl group resulting in two unequivalent carboxyl oxygen atoms. Between 1270 and 1150 cm^{-1} the phosphorylation spectra show a negative and a positive band which may be attributed to the disappearance of the $> PO_2^-$ group. Below 1200 cm^{-1}, several bands appear in the $Ca_2E_1 \rightarrow Ca_2E_1P$-spectra, but it is unclear whether or not they can be attributed to the phosphorylation reaction.

Several bands of the ADP-binding-spectra are still observed in the $Ca_2E_1 \rightarrow Ca_2E_1P$-spectra, supporting our assumption that ATP is bound to the phosphoenzyme under the conditions of our experiments.

4.8. Band assignment for the $Ca_2E_1P \rightarrow E_2P$-spectra

The bold lines in Fig. 8 show the difference between the $Ca_2E_1 \rightarrow Ca_2E_1P$-spectra and the $Ca_2E_1 \rightarrow E_2P$-spectra reflecting step (5) in Fig. 1B. These difference spectra show absorbance changes associated with phosphoenzyme conversion and Ca^{2+}-release and are therefore termed $Ca_2E_1P \rightarrow E_2P$-spectra. For a detailed band assignment, the reader is referred to the preceding discussion of the ADP-binding-spectra. However, some bands will be discussed here: The bands at 1750 and 1704 cm^{-1} can be assigned to C = O carboxyl groups which are free (1750 cm^{-1}) and strongly hydrogen bonded (1704 cm^{-1}), respectively. The bands can arise from protonation of COO^- groups or from breaking and weakening of strong hydrogen bonds to a C = O carboxyl group absorbing at lower wavenumbers. Indeed, there is a negative band at 1690 cm^{-1} in H_2O and 1678 cm^{-1} in ^2H_2O, which can be tentatively assigned to a strongly hydrogen bonded C = O group. However, this C = O mode may also be assigned to β-sheet or β-turn structures as well as to side chains of Gln or Asn.

In the region between 1670 and 1650 cm^{-1} only small band shifts are observed upon deuteration. This supports an assignment to amide I vibrations of the polypeptide backbone or to amino acid side chains inaccessible for deuteration.

Between 1640 and 1610 cm^{-1}, clear differences are observed between the spectra in H_2O and ^2H_2O. The strongest positive band in H_2O absorbs at 1638 cm^{-1} and in ^2H_2O at 1616 cm^{-1}. The most simple explana-

tion, a shift from 1638 to 1616 cm^{-1}, has to be rejected, since it is too large for an amide I band and too small for side group absorptions of Arg and Lys. A probable explanation is that both bands are present in H_2O and ^2H_2O, but superimposed by a negative band absorbing around 1620 cm^{-1} in H_2O, which is shifting to approx. 1630 cm^{-1} in ^2H_2O. If this is correct, the negative band can be assigned to carboxyl groups and the positive bands to β-sheet structures.

At 1570/1554 cm^{-1} and 1416/1398 cm^{-1}, two difference bands that can be assigned to carboxyl groups are observed most clearly in ^2H_2O. These signals were also observed in model spectra for Ca^{2+}-release with the model compounds free 'EDTA' and 'EDTA · Ca^{2+}' [6].

4.9. Interpretation of the $Ca_2E_1P \rightarrow E_2P$-spectra

Several processes [1] give rise to the $Ca_2E_1P \rightarrow E_2P$-spectra: (i) Reorientation of the Ca^{2+} binding sites to the luminal side, (ii) Ca^{2+}-release, (iii) change of substrate specifity for the dephosphorylation reaction, (iv) protection of the catalytic site from the solvent [18,19] and (v) the coupling between the processes at the phosphorylation site and the Ca^{2+} binding sites.

A pair of difference signals can be attributed to Ca^{2+}-release from carboxyl groups. The bands at 1750 and 1704 cm^{-1} may indicate protonation of carboxyl groups, a process which is expected to occur after Ca^{2+}-release since Ca^{2+} competes with H^+ for binding to the high affinity sites [48]. The positive 1750 cm^{-1} carboxyl band may also be discussed in connection with breaking of hydrogen bonds due to the protection of the catalytic site from the solvent leading to a more hydrophobic environment. At 1374/1352 cm^{-1} (best seen in ^2H_2O, Fig. 8B) and 1314/1292 cm^{-1} (best seen in H_2O, Fig. 8A), pairs of difference bands are found that may indicate breaking of hydrogen bonds to the nitrogen atoms of adenine. However, for other adenine bands sensitive to hydrogen bonding, the characteristic band shifts were not observed.

It is unlikely that lipid head groups play a role in phosphoenzyme conversion and Ca^{2+}-release, since no absorbance changes in the maximum of lipid absorption at 1736 cm^{-1} were observed. We thus conclude that the phosphoenzyme conversion does not have a strong impact on the structure and arrangement of the surrounding lipids.

4.10. Conformational changes upon nucleotide binding, phosphorylation and $Ca_2E_1P \rightarrow E_2P$ conversion

ATPase-nucleotide-bands in the region of amide I absorption allow to estimate the conformational changes in the ATPase polypeptide backbone in the course of nucleotide binding and phosphorylation. The difference bands are very small corresponding to at most 0.6% of the protein absorbance in this region.

IR and circular dichroism spectra of proteins in different states are mostly interpreted in terms of changes of the relative portions of secondary structures. In a crude model, let us therefore assume that several amino acids change their participation in a certain secondary structure during a protein reaction. If followed by IR spectroscopy this should lead to the disappearance of a band characteristic for the existing secondary structure and to the appearance of a band characteristic for the new structure. From the absorbance change of the strongest positive bands (at 1652 and 1626 cm^{-1}, $Ca_2E_1 \rightarrow E_2P$-(+Me_2SO)-spectra in ^2H_2O, Fig. 7), the extinction coefficient of amide I absorption and the ATPase content of our samples (see Experimental procedures section), we estimate the number of amino acids which contribute to these bands to be around six. This would imply that not more than six amino acids – corresponding to 0.6% of the total number – experience a net change of their secondary structure character.

In spite of this estimation, we think that a better interpretation of our spectra are small structural modifications within the existing secondary structure, which lead to band shifts and intensity changes. The number of amino acids involved here cannot be estimated easily.

A redistribution of approx. 8% of protein mass from the cytoplasmic region into the membrane bilayer upon phosphorylation of the ATPase to Ca_2E_1P was estimated from X-ray diffraction data [49]. In order to reconcile this with our spectra, we would have to assume that small modifications of bond angles and bond distances in the polypeptide backbone lead to large movements of extended parts of the protein.

4.11. Comparison with other IR investigations

The $Ca_2E_1 \rightarrow E_2P$-spectra in ^2H_2O (Fig. 7C) can be compared with results from other authors using deconvolution procedures of absorbance spectra to detect differences in the band composition of the amide I and amide II absorption. Arrondo et al. [50] have detected two bands at 1717 and 1677 cm^{-1} that do appear in the Ca_2E_1 state, but not in an E_2P-like state. Two bands at 1650 and 1537 cm^{-1} are characteristic for the E_2P-like state. In addition, they observe modifications at 1741 and 1731 cm^{-1}. In our $Ca_2E_1 \rightarrow E_2P$-spectra (Fig. 7C), bands characteristic for the Ca_2E_1-state appear negative and bands characteristic for the E_2P-state appear positive. Our spectra confirm only two of these bands at 1677 and 1650 cm^{-1}, and show a large number of bands that were not detected by Arrondo et al. [50]. Part of the discrepancies may arise from differences between the E_2P-like-state of [50] and the E_2P-

state that accumulates in our $Ca_2E_1 \rightarrow E_2P$-($+Me_2SO$)-samples. Other authors who also used deconvolution techniques did not find differences between the two states of the ATPase [7,51].

The $Ca_2E_1P \rightarrow E_2P$-($+Me_2SO$)-spectra of phosphoenzyme conversion and Ca^{2+} release in ^2H_2O reported here can be compared to difference spectra of Ca^{2+}-binding by the ATPase obtained by [52]. These authors used the photolytic release of Ca^{2+} from the photolabile chelator Nitr-5. Ca^{2+}-binding leads to negative bands at 1750, 1705, 1653, 1620, 1590, and 1550 cm^{-1}, as well as to positive bands at 1677, 1663, 1644 and 1632 cm^{-1}. After addition of dithiothreitol, they observe only the bands at 1677, 1663, 1653, 1633 and 1580 cm^{-1}. Nearly all of these bands have the same position in our $Ca_2E_1P \rightarrow E_2P$-spectra or $Ca_2E_1 \rightarrow E_2P$-spectra, but are of opposite sign. This indicates that structural changes due to Ca^{2+}-binding are reversed during the following reaction to E_2P.

5. Conclusions

Photolytic release of ATP or ADP allowed us to detect very small changes of ATPase-nucleotide IR-absorption associated with nucleotide binding, ATPase phosphorylation and phosphoenzyme conversion. The difference spectra obtained are characteristic for the individual transitions and exhibit highly detailed band structures which reflect the molecular processes underlying the individual steps.

Although we are able to attribute a number of bands to changes of peptide absorption, the overall conformational changes appear to be small; we favor an interpretation in terms of small modifications within the existing secondary structure and in terms of amino acid side chain rearrangements, rather than in terms of a reorganization of entire protein domains.

The photolytic release of substrates used here to generate the IR difference spectra is still in its infancy, and advantages (like the instantaneous triggering and the high sensitivity) and disadvantages (the generation of a difference spectrum by the triggering reaction itself) are evident. Nevertheless, it appears that with the development of further 'cages', taylored specifically for IR spectroscopy, this technique will become applicable to a wide range of enzyme reactions.

Acknowledgements

The authors would like to thank Prof. W. Hasselbach and Prof. R.S. Goody (Max-Planck-Institut, Heidelberg, Germany) for generous gifts of Ca^{2+}-ATPase and caged ADP. W.M. gratefully acknowledges a Heisenberg fellowship from the Deutsche Forschungsgemeinschaft.

References

[1] Andersen, J.P. (1989) Biochim. Biophys. Acta 988, 47–72.
[2] Barth, A., Mäntele, W. and Kreutz, W. (1991) Biochim. Biophys. Acta 1057, 115–123.
[3] Barth, Mäntele, W. and Kreutz, W. (1990) FEBS Lett. 277, 147–150.
[4] De Meis, L. and Hasselbach, W. (1971) J. Biol. Chem. 246, 4759–4763.
[5] The, R. and Hasselbach, W. (1977) Eur. J. Biochem. 74, 611–621.
[6] Barth, A. (1992) PhD Thesis, University of Freiburg.
[7] Buchet, R., Carrier, D., Wong, P.T.T., Jona, I. and Martonosi, A. (1990) Biochim. Biophys. Acta 1023, 107–118.
[8] Shigekawa, M., Wakabayashi, S. and Nakamura, H. (1983) J. Biol. Chem. 258, 14157–14161.
[9] Shigekawa, M. and Dougherty, J.P. (1978) J. Biol. Chem. 253, 1451–1457.
[10] Nakamura, Y. and Tonomura, Y. (1982) J. Biochem. 91, 449–461.
[11] Pickart, C.M. and Jencks, W.P. (1984) J. Biol. Chem. 259, 1629–1643.
[12] Shigekawa, M., Dougherty, J.P. and Katz, A.M. (1978) J. Biol. Chem. 253, 1442–1450.
[13] Teruel, J.A. and Inesi, G. (1988) Biochemistry 27, 5885–5890.
[14] Takisawa, H. and Tonomura, Y. (1979) J. Biochem. 86, 425–441.
[15] Shigekawa, M. and Dougherty, J.P. (1978) J. Biol. Chem. 253, 1458–1464.
[16] Shigekawa, M., Wakabayashi, S. and Nakamura, H. (1983) J. Biol. Chem. 258, 8698–8707.
[17] De Meis, L., Martins, O.B. and Alves, E.W. (1980) Biochemistry 19, 4253–4261.
[18] Nakamoto, R.K. and Inesi, G. (1984) J. Biol. Chem. 259, 2961–2970.
[19] Dupont, Y. and Pougeois, R. (1983) FEBS Lett. 156, 93–98.
[20] Champeil, P., Riollet, S., Orlowski, S., Guillain, F., Seebregts, C.J. and McIntosh, D.B. (1988) J. Biol. Chem. 263, 12288–12294.
[21] Jencks, W.P. (1969) in Catalysis in Chemistry and Enzymology, McGraw-Hill, New York.
[22] Bamford, C.H. and Tipper, C.F.H. (1977) in Comprehensive Chemical Kinetics, Elsevier Scientific, Amsterdam.
[23] Colthup, N.B., Daly, L.H. and Wiberley, S.E. (1975) in Introduction to Infrared and Raman Spectroscopy, Academic Press, New York.
[24] Venyaminov, S.Y. and Kalnin, N.N. (1990) Biopolymers 30, 1259–1271.
[25] Chirgadze, Y.N., Fedorov, O.V. and Trushina, N.P. (1975) Biopolymers 14, 679–694.
[26] Byler, D.M. and Susi, H. (1986) Biopolymers 25, 469–487.
[27] Susi, H., Timasheff, N. and Stevens, L. (1967) J. Biol. Chem. 242, 5460–5466.
[28] Chirgadze, Y.N. and Brazhnikov, E.V. (1974) Biopolymers 13, 1701–1712.
[29] Venyaminov, S.Y. and Kalnin, N.N. (1990) Biopolymers 30, 1243–1257.
[30] Chirgadze, Y.N., Shestopalov, B.V. and Venyaminov, S.Y. (1973) Biopolymers 12, 1337–1351.
[31] Toyama, A., Takeuchi, H. and Harada, I. (1991) J. Mol. Struct. 242, 87–98.
[32] Pinchas, S. and Laulicht, I. (1971) in Infrared Spectra of Labelled Compounds, Academic Press, London.
[33] Nakamoto, K. (1978) in Infrared and Raman Spectra of Inorganic and Coordination Compounds, John Wiley, New York.

[34] Rothschild, K.J., He, Y.W., Gray, D., Roepe, P.D., Pelletier, S.L., Brown, R.S., Herzfeld, J. (1989) Proc. Natl. Acad. Sci. USA 86, 9832–9835.
[35] Gerwert, K., Hess, B., Engelhard, M. (1990) FEBS Lett. 261, 449–454.
[36] Pohle, W., Bohl, M. and Böhlig, H. (1990) J. Mol. Struct. 242, 333–342.
[37] Shimanouchi, T., Tsuboi, M. and Kyogoku, Y. (1964) in Advances in Chemical Physics (Duchesne, J., ed.), pp. 435–498, Wiley – Interscience, New York.
[38] Feofanov, A.V., Efremov, R.G., Dzhandzhugazyan, K.N. and Nabiev, I.R. (1990) Biol. Membr. 7, 341–351.
[39] Hol, W.G.J., Van Duijnen, P.T. and Berendsen, H.J.C. (1978) Nature 273, 443–446.
[40] Taylor, W.R. and Green, N.M. (1989) Eur. J. Biochem. 179, 241–248.
[41] Lacapere, J.-J., Bennett, N., Dupont, Y. and Guillain, F. (1990) J. Biol. Chem. 265, 348–353.
[42] Stahl, N. and Jencks, W.P. (1987) Biochemistry 26, 7654–7667.
[43] Wakabayashi, S. and Shigekawa, M. (1990) Biochemistry 29, 7309–7318.
[44] Lacapere, J.-J. and Guillain, F. (1990) J. Biol. Chem. 265, 8583–8589.
[45] Dupont, Y., Pougeois, R., Ronjat, M. and Verjovski-Almeida, S. (1985) J. Biol. Chem. 7249, 7241–7249.
[46] Coll, R.J. and Murphy, A.J. (1991) Biochemistry 30, 1456–1461.
[47] Bellamy, L.J. and Beecher, L. (1952) J. Chem. Soc. 475–483.
[48] Fernandez-Belda, F., Garcia-Carmona, F. and Inesi, G. (1988) Arch. Biochem. Biophys. 260, 118–124.
[49] Blasie, J.K., Herbette, L.G., Pascolini, D., Skita, V., Pierce, D.H. and Scarpa, A. (1985) Biophys. J. 48, 9–18.
[50] Arrondo, J.L.R., Mantsch, H.H., Mullner, N., Pikula, S. and Martonosi, A. (1987) J. Biol. Chem. 262, 9037–9043.
[51] Villalain, J., Gomez-Fernandez, J.C., Jackson, M. and Chapman, D. (1989) Biochim. Biophys. Acta 978, 305–312.
[52] Buchet, R., Jona, I. and Martonosi, A. (1991) Biochim. Biophys. Acta 1069, 209–217.
[53] Inesi, G. and De Meis, L. (1985) in The Enzymes of Biological Membranes, Vol. 3 (Martonosi, A., ed.), pp. 157–191, Plenum Press, New York.
[54] De Meis, L. and Vianna, A. (1979) Annu. Rev. Biochem. 48, 275–292.